HHS Public Access

Author manuscript

Tuberculosis (Edinb). Author manuscript; available in PMC 2016 May 01.

Published in final edited form as:

Tuberculosis (Edinb). 2015 May ; 95(3): 251–258. doi:10.1016/j.tube.2015.03.005.

MadR1, a *Mycobacterium tuberculosis* cell cycle stress response protein that is a member of a widely conserved protein class of prokaryotic, eukaryotic and archaeal origin

Rebecca Crew[a,b], **Melissa V. Ramirez**[a], **Kathleen England**[c], and **Richard A. Slayden**[a,‡]

Rebecca Crew: Rebecca.crew@colostate.edu; Melissa V. Ramirez: Melissa.ramirez@colostate.edu; Kathleen England: englandk@stanford.edu; Richard A. Slayden: Richard.slayden@colostate.edu

[a]Mycobacteria Research Laboratories, Department of Microbiology, Immunology and Pathology, Colorado State University, Fort Collins, CO 80523, USA

SUMMARY

Stress-induced molecular programs designed to stall division progression are nearly ubiquitous in bacteria, with one well-known example being the participation of the SulA septum inhibiting protein in the SOS DNA damage repair response. Mycobacteria similarly demonstrate stress-altered growth kinetics, however no such regulators have been found in these organisms. We therefore set out to identify SulA-like regulatory proteins in *Mycobacterium tuberculosis*. A bioinformatics modeling-based approach led to the identification of *rv2216* as encoding for a protein with weak similarity to SulA, further analysis distinguished this protein as belonging to a group of previously uncharacterized growth promoting proteins. We have named the mycobacterial protein encoded by *rv2216* morphology altering division regulator protein 1, MadR1. Overexpression of *madR1* modulated cell length while maintaining growth kinetics similar to wild-type, and increased the proportion of bent or V-form cells in the population. The presence of MadR1-GFP at regions of cellular elongation (poles) and morphological differentiation (V-form) suggests MadR1 involvement in phenotypic herterogeneity and longitudinal cellular growth. Global transcriptional analysis indicated that MadR1 functionality is linked to lipid editing programs required for growth and persistence. This is the first report to differentiate the larger class of these conserved proteins from SulA proteins and characterizes MadR1 effects on the mycobacterial cell.

[‡]Author to whom correspondence should be addressed: Richard A. Slayden, Department of Microbiology, Immunology and Pathology, Colorado State University, Fort Collins, CO 80523-0092.

[b]Current address: Bacterial Diseases Branch, Division of Vector-Borne Diseases, National Center for Emerging and Zoonotic Infectious Diseases, The Centers for Disease Control and Progression, Fort Collins, CO 80523, USA

[c]Current address: Stanford University School of Medicine, Department of Infectious Diseases, Stanford, CA 94305, USA

AUTHOR'S CONTRIBUTIONS

RC performed the bioinformatic analysis, growth kinetics, ultrastructural analysis and fluorescent microscopy. MVR aided in data analysis and growth kinetic study. KE carried out the MMC treatment, SEM and transcriptional studies. RAS coordinated the laboratory activities. All authors aided in drafting and editing and have approved the final manuscript.

Keywords

Mycobacterium tuberculosis; rv2216; MadR1; cell division; cell cycle regulation

1. INTRODUCTION

A hallmark of *Mycobacterium tuberculosis* (*Mtb*) is its ability to evade host responses, survive stress conditions and tolerate drug treatment, resulting in the establishment and maintenance of a latent state of infection for long durations [1–3]. Studies of *Mtb* grown in artificial stress conditions and in animal models of infection as well as evidence from patient tissues substantiate that the bacilli can survive stresses by entering into a quasi-dormant state often referred to as non-replicating persistence (NRP). Despite the prominent role these bacteria have played in global disease, the regulatory elements controlling replication remain poorly understood, particularly in relation to stress-induced NRP.

Mounting experimental evidence indicates that the bacterial response to stress includes regulatory elements that govern cell division and alter morphology [4]. In other bacterial species, SOS response proteins, such as SulA (SfiA) in *Escherichia coli* and YneA in *Bacillus subtilis*, are known to regulate cell division and induce filamentation in response to drug exposure, DNA damage, radiation, or reactive oxidative intermediates [5–6]. These stress responsive regulatory proteins are used in a final survival strategy to halt cells until favorable growth conditions exist.

Mtb bacilli are known to filament following phagocytosis by host macrophages and under *in vitro* stress models of NRP, yet the underlying mechanisms facilitating these growth transitions remain unknown [3, 7]. It was recently found that the Ssd and Soj_{Mtb} proteins induce cellular survival responses coupling filamentation with the induction of adaptive metabolic programs, demonstrating the association between these processes that are important characteristics of persistent mycobacterial infections [8–9]. However, evidence does not support a role for Ssd as the direct modulator of division progression through control of FtsZ protein polymerization dynamics, as has been shown for SulA and several other stress-associated division inhibitors [6, 8, 10]. Currently no genes encoding a protein known to directly participate in division cessation through septum control have been identified in any mycobacterial genome, raising the question as to how *Mtb* regulates cell cycle progression characterized by filamentation and transition into NRP during the establishment of a persistent infection.

To better understand the regulatory mechanisms controlling growth and division in mycobacteria, we set out to identify unannotated cell division regulatory proteins involved in division progression using consensus-modeling bioinformatics, morphological analysis, protein mapping and transcriptional analysis. This approach led to the identification of *rv2216* that encodes a SulA-like protein, and further analysis revealed that Rv2216 belongs to a group of widely conserved but previously uncharacterized growth promoting proteins of prokaryotic, eukaryotic and archaeal origin, which we have named morphology altering division regulator protein 1 (MadR1). We show that MadR1 of *Mtb* contributes to morphological heterogeneity and affects elongation but not division. Furthermore, *madR1*

overexpression induced a global transcriptional response promoting persistence-linked lipid metabolism at the plasma membrane. This is the first report defining the novel class of MadR1 proteins and characterizing their phenotypic effects in mycobacteria.

2. METHODS

2.1. Strains, growth and SEM

Mtb H37Rv and *Mycobacterium smegmatis* MC_2 155 were grown at 37°C in Middlebrook 7H9 liquid medium or on 7H11 agar media supplemented with 25 μg ml^{-1} Kanamycin sulfate when necessary [9]. *Mtb* H37Rv was grown to an $O.D._{600nm}$ of 0.1 – 0.2 and subjected to continued growth in the presence of Mitomycin C (MMC) at 0.2 μg ml^{-1} 100 μl total volumes. IC_{50} was performed in triplicate and was defined as the concentration of drug required to reduce bacterial growth 50% after 7-days incubation [11]. Viability testing was performed at 1, 3, and 5 days post-treatment with 0.2 μg ml^{-1} or 0.1 μg ml^{-1} MMC by determining colony forming units via direct plating and outgrowth. *Rv2216* [EMBL accession no. **CCP44993**] was cloned into the mycobacterial vector pVV16 and transformed into *M. smegmatis* and *Mtb* as described elsewhere [9]. For ultrastructural analysis, *M. smegmatis* cells overexpressing *madR1* were collected at mid-log growth then prepared and imaged as previously described [8]. The relative proportion of linear and V-form morphologies were tallied for 100 cells per field of view, and averaged for five different views per condition.

2.2. Bioinformatic and statistical analysis

Datasets of annotated SulA and MadR1 proteins were created from the UniProt and OMA Browser databases and aligned using the MafftWS global sequence alignment tool through Jalview V2.7 [12]. Aligned datasets were used to build Hidden Markov Models (HMMs) with HMMER tools and then used to search encoded *Mtb* proteins containing SulA-like motifs. BLASTX, BLASTP, and TBLASTN analysis against searchable databases prepared from prototype protein datasets were also used. Alignment and dendogram construction performed through Jalview [12]. Alignment quality scores indicate probability that observed amino acids in an aligned column are the result of conservation; lower scores indicate good potential for mutation and higher scores posing less cost. Distance values are the sum of the BLOSUM62 scores for each residue pair in the original multialignment, and are minimized using a Neighbor Joining algorithm. Tools from the EMBOSS package were used to analyze the proteins and datasets [13]. Functional enrichment calculations were performed through the Tuberculosis Database (www.tbdb.org) using the *MadR1* overexpression dataset obtained by microarray.

2.3. Transcriptional profiling

Cells were harvested at mid-log, resuspended in TRIzol reagent (Invitrogen™), and total RNA was liberated by physical disruption [14]. cDNA was generated from total RNA using the SuperScript™ III First-Strand Synthesis System for RT-PCR (Invitrogen™). Primer sequences (Additional file 4). And quantitative real-time PCR was performed as previously described [8]. Quantification of each gene was determined relative to a time zero, normalized to *sigA* reference gene expression and log base 2 transformed. Microarray

analysis was performed with labeled cDNA generated using direct labeling from 5 μg of total RNA [15]. The resulting fluorescence for each channel of the array (Cy3 and Cy5) was normalized to the mean channel intensity and analyzed using ANOVA single factor analysis. Significance was considered to be a >2-fold alteration in expression, with *p*-value of <0.05.

2.4. Fluorescent microscopy

An extrachromosomal *E. coli*-mycobacteria shuttle vector, pMCSU7, was developed for the inducible expression of fluorescently tagged protein using the *S. coelicolor tetO* promoter from tcp3 (Additional file 5). The *MadR1* coding sequence was PCR amplified from H37Rv genomic DNA and combined into pMCSU7 using Gateway technology. Constructs were screened using DNA sequencing prior to transformation into electrocompetent *M. smegmatis*. Mid-log grown transformants were diluted to $O.D._{600nm}$ 0.2 and expression was induced in the dark for 6 hours using 50 ng ml^{-1} anhydrotetracycline (Clontech). Cells were stained with FM 4-64 Fx in HBSS (Invitrogen™), fixed in 4% paraformaldehyde, applied to glass slides, and coated with Vectashield Hard Set with DAPI (Vector Laboratories). Slides were stored at 4C for a maximum of 24 hours before imaging at 1000x magnification using an inverted, oil-immersion Olympus IX71 microscope with a Retiga 2000R camera (QImaging) and Slidebook software (Intelligent Imaging Innovations Inc.).

3. RESULTS

3.1. Identification of the SulA-like MadR1 protein encoded by *rv2216*

A putative cell division regulatory protein in *Mtb* was identified using a reciprocal best-hit (RBH) strategy constructed from local and global Hidden Markov Models (HMMs) of annotated SulA proteins from 85 bacterial genomes built from the OMA 415268 dataset [16]. BLAST searches using the SulA consensus model against the H37Rv proteome identified a 301 amino acid protein, encoded by *rv2216*, annotated as a conserved hypothetical protein of unknown function. Domain mapping through Sanger-Pfam revealed a SulA-like epimerase/dehydratase domain [Pfam accession no. **PF01370**] toward the N-terminus, followed by a domain of unknown function [Pfam accession no. **PF08338**] not traditionally associated with SulA proteins (Figure 1A) [17]. In addition, there is a notable difference in length between SulA-family (135–170 amino acids in length) and Rv2216 (301 amino acids in length) and alignment of Rv2216 showed 33% similarity with only 9% coverage to SulA proteins. Consensus modeling revealed that Rv2216 is a member of a loosely defined yet highly conserved family of hypothetical proteins implicated in cell division regulation due to their weak similarity to SulA. Notably, Rv2216 groups with proteins in OMA groups 59319 and 55637, that include members from various prokaryotic, eukaryotic and archaeal origins, and display an extraordinary level of conservation at the sequence level (Figure 1C). A multialignment comparing a selection of bacterial SulA protein sequences with the archaeal, prokaryotic and eukaryotic sequences was used to generate a phylogenetic tree with the shortest possible branch lengths (Figure 1B). The protein sequences from distantly related organisms map to a separate clade from the bacterial SulA proteins further demonstrating that distinct sequence features separate these two protein families and that an exceptional level of sequence conservation may be observed for these conserved MadR1-like proteins across all kingdoms of life.

3.2 Overexpression of *madR1* alters cellular morphology and division symmetry

To assess the role of MadR1 in the regulation of cell growth, the effects of overexpression of *madR1* on morphology was examined in *M. smegmatis* and *M. tuberculosis* by scanning electron microscopy (SEM). The recombinant strain displayed moderate and bimodal cellular elongation, the majority measuring between 1.1–4 μm with a mean of 2.5 μm and minority measuring 4.1–6.3 μm with a mean of 5.1 μm, as compared to vector control, 1–3 μm and a mean of 1.9 μm (Figure 2A–D, G). Cellular elongation has previously been shown to indicate regulation of cell division, however no significant alterations were observed in division rates by monitoring optical density (data not shown) [8, 15, 18–19].

A portion of the mycobacterial merodiploid strains appear with V-form morphology, with the greatest proportion being present during logarithmic growth [20]. Specifically, the *M. smegmatis:madR1* merodiploid population displayed an increased proportion of cells adopting V-form morphologies (57.8%) compared to controls (27.6%) (Figure 2 A–B, E) that was found to be statistically significant by Pearson's chi-squared test with a p-value of 1.56e-5 during mid-log growth (Figure 2 F). Phenotypics of the mycobacterial merodiploid strains were similar, however only *M. smegmatis* strains were used for ultrastructural analysis due to increased clumping observed in the *Mtb* strain (Figure 2 C–D). Together, these observations suggest a role for MadR1 in cell growth relative to the rate of division and promoting the poorly understood bent morphologies in mycobacteria.

3.3. MadR1 is not a member of the mycobacterial SOS response induced by DNA damage

Since MadR1 shares sequence similarity with SulA, and SulA is a known component of the SOS response in other organisms, Mitomycin C (MMC) was used to produce DNA damage and induce the SOS response in *Mtb* as described previously [11]. The characterized SOS response in *Mtb* was successfully induced by MMC treatment, apparent by the increased expression levels of SOS-associated genes (Figure 3 A) and repression of division genes (Figure 3 B) compared to un-treated controls, as evaluated by quantitative reverse transcriptase PCR (qRT-PCR). However, *madR1* expression was not induced to a similar extent as SOS components, suggesting an alternative role and level of regulation for MadR1 compared to typical SOS-responsive proteins.

3.4. MadR1 overexpression induces adaptive metabolic programs associated with dormancy

Table 1 describes features of the MadR1 response in *Mtb* using Gene Ontology which provides a controlled vocabulary for the annotation of ORFs based upon three ontological descriptors: cellular component, biological process and molecular function. Unfortunately all three descriptors are not always possible, as in the case of MadR1 family proteins which have not been attributed a defined molecular function. To elucidate the potential functional ontology of MadR1 proteins Categories of Orthologous Groups (COGs), which uses a combination of phylogeny and orthology to group gene products into functional categories, and Pathway Ontology calculations that provide further detail of the indicated functions, were also included.

As shown in Table 1, the 178 genes showing a 2-fold or greater induction upon *madR1* overexpression show a strong association with growth and activities at the inner membrane. COG and Pathway annotations reveal a strong induction of secondary metabolism and lipid oxidation pathways, important components of alternative metabolism within the host, in addition to histidine biosynthesis and lactate oxidation, which are important for growth and anaerobic respiration. The 99 genes displaying significant down-regulation in the *madR1* merodiploid were similarly associated with the plasma membrane. The pathways most significantly repressed were involved in anaerobic respiration (other than lactate dehydrogenase) and the early steps of fatty acid biosynthesis and elongation, in addition to tryptophan biosynthesis. These associations support a role for MadR1 in growth and regulation at the plasma membrane and dormancy-associated stress responses that utilize alternative respiration and lipid turnover, such as those associated with hypoxia and reaeration.

3.5. MadR1-GFP localizes to regions of cell wall growth during *M. smegmatis* replication

To investigate the localization of MadR1 in context of the cell cycle, MadR1-GFP fusion protein, DNA and membranes were visualized by fluorescent microscopy. In general, MadR1 localized in a consistent pattern through differential phases of the division cycle (Figure 4). Following this scheme it appears that during early division events MadR1-GFP localizes at polar locations with minimal presence at the mid-cell site (Figure 4 B-i). The mid-cell presence wanes and the polar foci persist during the primary elongation phase (Figure 4 B-ii), displaying differential behavior at the early vertex of future V-form cells (Figure 4 B-ii arrowhead) compared to the linear cell. After formation of the septum MadR1-GFP relocates to a quarter-cell position (Figure 4 B-iii); a location representing an early division site for the next round of division. As the daughter cells begin to separate, marking the completion of a single round of division, the quarter-cell foci persist and the development of novel foci may be observed at the newly formed cell poles (Figure 4 B-iv). Presumably, after this point the mid-cell foci relocate to the old cell pole while the new foci become more prominent, and the cycle repeats from the beginning. Importantly, the regions of MadR1-GFP localization, including the poles and outer edge of the vertex in V-form cells, are the primary sites of cell wall growth and remodeling in mycobacteria.

4. DISCUSSION

The ability of *Mtb* to adapt via regulation of metabolism and cell cycle in response to alternative and stressful conditions is central to the establishment and maintenance of a persistent, latent infection [1–3]. However, while such regulators exist in other bacteria, few regulatory checkpoints have been described during normal or adaptive growth for *Mtb*. A bioinformatics investigation of putative regulators using consensus sequencing modeling revealed a potential cell cycle regulator that shares similarity with SulA, an SOS-responsive FtsZ inhibitor of cell division. However, the limited sequence similarity between MadR1 and SulA protein orthologs along with the assignment of MadR1 into OMA groups of conserved proteins with poorly defined functions presented a challenge to defining function in the complex regulatory networks employed by *Mtb* under acute infection, NRP and

relapse. Therefore, we designed a series of experiments to assess the function of the morphology asymmetric division regulator protein 1 (MadR1), encoded by *rv2216*.

Previous work in model bacteria has shown that SulA expression is induced in response to DNA damage, along with other classical components of the SOS response. While studies in mycobacteria using the known SOS inducer MMC mutagen reduced growth and induced known components associate with the SOS response, this treatment did not similarly induce *MadR1* expression [5–6, 10, 21–27]. This observation is indicates that MadR1 is not a primary component of the mycobacterial SOS response, but rather is involved in cell cycle regulation.

SEM and fluorescent microscopy showed the predominant bacterial morphology resulting from overexpression of MadR1 to be filamentous V-form cells lacking septal structures. The observation of V-form cells provided a foundation to investigate localization of MadR1 at different times of the cell cycle based on previous morphological studies [20, 28]. Aldridge *et al.* used single-cell time-lapse microscopy to observe the growth and division of a single mycobacterial cell through successive rounds of division revealing the early determination of a vertex near one pole of an elongating cell, with further elongation from that pole resulting in a V-form cell [29]. The use of this cell cycle progression scheme led to several important observations. Firstly, it is apparent that MadR1-GFP localization is dynamic in relation to the division cycle. Second, MadR1-GFP localization to the poles and outer edge of the vertex in V-form cells is consistent with participation in cell wall growth and remodeling, as these coincide with locations previously shown to be the exclusive regions of nascent peptidoglycan incorporation in mycobacterium by Van-Bodipy staining [20]. Third, MadR1-GFP foci frequently co-localize with FM 4–64 Fx styryl dye hotspots, which displays preferential staining for the anionic (acidic) bacterial lipids phosphatidylglycerol and cardiolipin [30]. The co-localization of MadR1-GFP foci and FM 4–64 Fx hotspots indicates a connection between MadR1 activity and anionic phospholipid domains. MadR1 may localize to pre-established domains for activation as has been observed for several other membrane-associated proteins, or may stimulate the production of acidic phospholipids [31–32]. It is possible these co-localized hotspots are due to the formation of lipid bodies resulting from protein overproduction or GFP fusion, however certain behaviors are unlikely to be attributed to lipid bodies. For example, the localization of MadR1-GFP foci observed along the outer edge of the vertex, displaying distinct foci, which appear to spread along the inner membrane at the outer bend, indicates a role for MadR1 in the development of bent daughter cells, as this phenomenon was not observed in the linear daughter cell. Importantly, the frequency of V-form cells nearly doubled upon *madR1* overexpression, substantiating MadR1 involvement in the regulation and development of the poorly understood V-form morphology. However, these conclusions should be as accepted cautiously since the *Mtb* coding sequence shares 82% similarity and 98% coverage with the ortholog from *M. smegmatis* in which it was overproduced, and since the behavior of proteins arising from exogenous fusion or overproduction systems may not accurately depict the activity of native proteins at physiologically relevant levels. It is unfortunate that attempts to knockout madR1 from mycobacteria were unsuccessful, likely due to its placement within an operon encoding several known essential proteins.

Global transcriptional profiling and pathway ontology analysis revealed a strong connection between over-expression of MadR1 and lipid β-oxidation and secondary metabolism attributed to the utilization of acetyl-CoA by the pyruvate dehydrogenase complex (PDH) following β-oxidation of fatty acids. This is consistent with the organization of *MadR1* within a polycistronic operon with the PDH component dihydrolipoamide acyltransferase (*dlaT*, *rv2215*) and the lipoate biosynthesis proteins *lipB* and *lipA* respectively (*rv2217-rv2218*). Operon partners LipA and LipB work in concert to specifically activate DlaT through a post-translational modification known as lipoylation [34–35]. Lipoylated DlaT then carries out its role as the E2 component of two separate multi-protein complexes in mycobacteria: 1) PDH, an essential component of intermediary metabolism, and 2) the peroxynitrite reductase/peroxidase complex (PNR/P) required for the neutralization of oxidizing species during infection and important for persistence within the host [36–37]. The induction of lipid catabolism and repression of lipid synthesis observed in the MadR1 response suggests lipid editing and turnover are taking place, corroborated by the specific induction of *tgs1* and *lipY*, encoded by *rv3130c* and *rv3097c*, the primary genes involved in triacylglycerol (TAG) biosynthesis and degradation respectively [38]. In *Mtb*, TAG accumulation is specifically linked with pathological conditions associated with host infection and dormancy phenotypes where it is suspected to serve as an important energy source within host tissues [39]. Studies performed in *Saccharomyces cerevisiae* have shown an intimate connection between TAG and phospholipid metabolism, therefore the lipid recycling programs observed in the MadR1 response may serve as an efficient method to repair and reorganize membrane architecture of *Mtb* under energy-limiting conditions, such as those experienced within host tissues during prolonged infection [40–41]. Similar to conditions requiring DlaT activity, this functionality would be equally important during times of rapid growth and NRP. Together these studies demonstrate an indirect yet undeniable genetic and functional link between MadR1 and latent disease leading to reactivation.

5. CONCLUSIONS

We have deemed the *rv2216* gene product, MadR1 in *Mtb* based upon its unique cellular effects. MadR1 promotes the morphological heterogeneity that has been linked to survivability and induced adaptive metabolic programs associated with NRP and cell wall maintenance. Currently MadR1 is the only protein shown to the unique and poorly understood mycobacterial V-form and morphological asymmetry, which is in agreement with a newly evolving theme connecting programs that promote phenotypic diversity and alternative metabolism with survival within the host. Characterization of this *Mtb* protein and this family of conserved proteins provides a greater understanding of cellular division and morphological control in diverse organisms, which are believed to be the remnants of ancient unicellular symbionts [33, 42–44]. Importantly, the extensive level of conservation both at the organism and sequence level through millions of years of evolution suggests a vital role for MadR1 in the survival and propagation of diverse life forms.

Acknowledgments

We thank Dr. Dennis Knudson for bioinformatics support, Kerry Brookman for the design and development of pMCSU7 vector used in the fluorescent microscopy studies, and Dr. Alan Schenkel for aid with microscopy techniques. This work was funded by NIH Grant AI55298 to RAS.

RERERENCES

1. Rustad TR, Harrell MI, Liao R, Sherman DR. The enduring hypoxic response of Mycobacterium tuberculosis. PLoS ONE. 2008; 3(1):e1502. [PubMed: 18231589]
2. Betts JC, Lukey PT, Robb LC, McAdam RA, Duncan K. Evaluation of a nutrient starvation model of Mycobacterium tuberculosis persistence by gene and protein expression profiling. Mol Microbiol. 2002; 43(3):717–731. [PubMed: 11929527]
3. Wayne LG, Sohaskey CD. Nonreplicating persistence of mycobacterium tuberculosis. Annu Rev Microbiol. 2001; 55:139–163. [PubMed: 11544352]
4. Justice SS, Hunstad DA, Cegelski L, Hultgren SJ. Morphological plasticity as a bacterial survival strategy. Nat Rev Microbiol. 2008; 6(2):162–168. [PubMed: 18157153]
5. Kawai Y, Moriya S, Ogasawara N. Identification of a protein, YneA, responsible for cell division suppression during the SOS response in Bacillus subtilis. Mol Microbiol. 2003; 47(4):1113–1122. [PubMed: 12581363]
6. Trusca D, Scott S, Thompson C, Bramhill D. Bacterial SOS checkpoint protein SulA inhibits polymerization of purified FtsZ cell division protein. J Bacteriol. 1998; 180(15):3946–3953. [PubMed: 9683493]
7. Chauhan A, Madiraju MV, Fol M, Lofton H, Maloney E, Reynolds R, Rajagopalan M. Mycobacterium tuberculosis cells growing in macrophages are filamentous and deficient in FtsZ rings. J Bacteriol. 2006; 188(5):1856–1865. [PubMed: 16484196]
8. England K, Crew R, Slayden RA. Mycobacterium tuberculosis septum site determining protein, Ssd encoded by rv3660c, promotes filamentation and elicits an alternative metabolic and dormancy stress response. BMC Microbiol. 2011; 11:79. [PubMed: 21504606]
9. Ramirez MV, Dawson CC, Crew R, England K, Slayden RA. MazF6 toxin of Mycobacterium tuberculosis demonstrates antitoxin specificity and is coupled to regulation of cell growth by a Soj-like protein. BMC Microbiol. 2013; 13(1):240. [PubMed: 24172039]
10. Cordell SC, Robinson EJ, Lowe J. Crystal structure of the SOS cell division inhibitor SulA and in complex with FtsZ. Proc Natl Acad Sci U S A. 2003; 100(13):7889–7894. [PubMed: 12808143]
11. Dullaghan EM, Brooks PC, Davis EO. The role of multiple SOS boxes upstream of the Mycobacterium tuberculosis lexA gene--identification of a novel DNA-damage-inducible gene. Microbiology. 2002; 148(Pt 11):3609–3615. [PubMed: 12427951]
12. Waterhouse AM, Procter JB, Martin DM, Clamp M, Barton GJ. Jalview Version 2--a multiple sequence alignment editor and analysis workbench. Bioinformatics. 2009; 25(9):1189–1191. [PubMed: 19151095]
13. Rice P, Longden I, Bleasby A. EMBOSS: the European Molecular Biology Open Software Suite. Trends Genet. 2000; 16(6):276–277. [PubMed: 10827456]
14. Huang Q, Kirikae F, Kirikae T, Pepe A, Amin A, Respicio L, Slayden RA, Tonge PJ, Ojima I. Targeting FtsZ for antituberculosis drug discovery: noncytotoxic taxanes as novel antituberculosis agents. J Med Chem. 2006; 49(2):463–466. [PubMed: 16420032]
15. Slayden RA, Knudson DL, Belisle JT. Identification of cell cycle regulators in Mycobacterium tuberculosis by inhibition of septum formation and global transcriptional analysis. Microbiology. 2006; 152(Pt 6):1789–1797. [PubMed: 16735741]
16. Altenhoff AM, Schneider A, Gonnet GH, Dessimoz C. OMA 2011: orthology inference among 1000 complete genomes. Nucleic Acids Res. 2011; 39(Database issue):D289–294. [PubMed: 21113020]
17. Punta M, Coggill PC, Eberhardt RY, Mistry J, Tate J, Boursnell C, Pang N, Forslund K, Ceric G, Clements J, et al. The Pfam protein families database. Nucleic Acids Res. 2012; 40(Database issue):D290–301. [PubMed: 22127870]

18. Respicio L, Nair PA, Huang Q, Anil B, Tracz S, Truglio JJ, Kisker C, Raleigh DP, Ojima I, Knudson DL, et al. Characterizing septum inhibition in Mycobacterium tuberculosis for novel drug discovery. Tuberculosis (Edinb). 2008; 88(5):420–429. [PubMed: 18479968]
19. Slayden RA, Belisle JT. Morphological features and signature gene response elicited by inactivation of FtsI in Mycobacterium tuberculosis. J Antimicrob Chemother. 2008
20. Thanky NR, Young DB, Robertson BD. Unusual features of the cell cycle in mycobacteria: polar-restricted growth and the snapping-model of cell division. Tuberculosis (Edinb). 2007; 87(3):231–236. [PubMed: 17287144]
21. Janion C. Inducible SOS response system of DNA repair and mutagenesis in Escherichia coli. Int J Biol Sci. 2008; 4(6):338–344. [PubMed: 18825275]
22. Au N, Kuester-Schoeck E, Mandava V, Bothwell LE, Canny SP, Chachu K, Colavito SA, Fuller SN, Groban ES, Hensley LA, et al. Genetic composition of the Bacillus subtilis SOS system. J Bacteriol. 2005; 187(22):7655–7666. [PubMed: 16267290]
23. Hill TM, Sharma B, Valjavec-Gratian M, Smith J. sfi-independent filamentation in Escherichia coli Is lexA dependent and requires DNA damage for induction. J Bacteriol. 1997; 179(6):1931–1939. [PubMed: 9068638]
24. Kuzminov A. Recombinational repair of DNA damage in Escherichia coli and bacteriophage lambda. Microbiol Mol Biol Rev. 1999; 63(4):751–813. table of contents. [PubMed: 10585965]
25. Schoemaker JM, Gayda RC, Markovitz A. Regulation of cell division in Escherichia coli: SOS induction and cellular location of the sulA protein, a key to lon-associated filamentation and death. J Bacteriol. 1984; 158(2):551–561. [PubMed: 6327610]
26. Maguin E, Brody H, Hill CW, D'Ari R. SOS-associated division inhibition gene sfiC is part of excisable element e14 in Escherichia coli. J Bacteriol. 1986; 168(1):464–466. [PubMed: 3531184]
27. Maguin E, Lutkenhaus J, D'Ari R. Reversibility of SOS-associated division inhibition in Escherichia coli. J Bacteriol. 1986; 166(3):733–738. [PubMed: 3011740]
28. Dahl JL. Electron microscopy analysis of Mycobacterium tuberculosis cell division. FEMS Microbiol Lett. 2004; 240(1):15–20. [PubMed: 15500974]
29. Aldridge BB, Fernandez-Suarez M, Heller D, Ambravaneswaran V, Irimia D, Toner M, Fortune SM. Asymmetry and aging of mycobacterial cells lead to variable growth and antibiotic susceptibility. Science. 2012; 335(6064):100–104. [PubMed: 22174129]
30. Barak I, Muchova K. The role of lipid domains in bacterial cell processes. Int J Mol Sci. 2013; 14(2):4050–4065. [PubMed: 23429192]
31. Erez E, Stjepanovic G, Zelazny AM, Brugger B, Sinning I, Bibi E. Genetic evidence for functional interaction of the Escherichia coli signal recognition particle receptor with acidic lipids in vivo. J Biol Chem. 2010; 285(52):40508–40514. [PubMed: 20956528]
32. Mazor S, Regev T, Mileykovskaya E, Margolin W, Dowhan W, Fishov I. Mutual effects of MinD-membrane interaction: II. Domain structure of the membrane enhances MinD binding. Biochim Biophys Acta. 2008; 1778(11):2505–2511. [PubMed: 18760260]
33. Maple J, Fujiwara MT, Kitahata N, Lawson T, Baker NR, Yoshida S, Moller SG. GIANT CHLOROPLAST 1 is essential for correct plastid division in Arabidopsis. Curr Biol. 2004; 14(9): 776–781. [PubMed: 15120068]
34. Spalding MD, Prigge ST. Lipoic acid metabolism in microbial pathogens. Microbiol Mol Biol Rev. 2010; 74(2):200–228. [PubMed: 20508247]
35. Shi S, Ehrt S. Dihydrolipoamide acyltransferase is critical for Mycobacterium tuberculosis pathogenesis. Infect Immun. 2006; 74(1):56–63. [PubMed: 16368957]
36. Tian J, Bryk R, Shi S, Erdjument-Bromage H, Tempst P, Nathan C. Mycobacterium tuberculosis appears to lack alpha-ketoglutarate dehydrogenase and encodes pyruvate dehydrogenase in widely separated genes. Mol Microbiol. 2005; 57(3):859–868. [PubMed: 16045627]
37. Bryk R, Lima CD, Erdjument-Bromage H, Tempst P, Nathan C. Metabolic enzymes of mycobacteria linked to antioxidant defense by a thioredoxin-like protein. Science. 2002; 295(5557):1073–1077. [PubMed: 11799204]
38. Deb C, Daniel J, Sirakova TD, Abomoelak B, Dubey VS, Kolattukudy PE. A novel lipase belonging to the hormone-sensitive lipase family induced under starvation to utilize stored

triacylglycerol in Mycobacterium tuberculosis. J Biol Chem. 2006; 281(7):3866–3875. [PubMed: 16354661]

39. Daniel J, Maamar H, Deb C, Sirakova TD, Kolattukudy PE. Mycobacterium tuberculosis uses host triacylglycerol to accumulate lipid droplets and acquires a dormancy-like phenotype in lipid-loaded macrophages. PLoS Pathog. 2011; 7(6):e1002093. [PubMed: 21731490]
40. Mora G, Scharnewski M, Fulda M. Neutral lipid metabolism influences phospholipid synthesis and deacylation in Saccharomyces cerevisiae. PLoS ONE. 2012; 7(11):e49269. [PubMed: 23139841]
41. Gaspar ML, Hofbauer HF, Kohlwein SD, Henry SA. Coordination of storage lipid synthesis and membrane biogenesis: evidence for cross-talk between triacylglycerol metabolism and phosphatidylinositol synthesis. J Biol Chem. 2011; 286(3):1696–1708. [PubMed: 20972264]
42. Raynaud C, Cassier-Chauvat C, Perennes C, Bergounioux C. An Arabidopsis homolog of the bacterial cell division inhibitor SulA is involved in plastid division. Plant Cell. 2004; 16(7):1801–1811. [PubMed: 15208387]
43. Gallwitz M, Reimer JM, Hellman L. Expansion of the mast cell chymase locus over the past 200 million years of mammalian evolution. Immunogenetics. 2006; 58(8):655–669. [PubMed: 16807745]
44. Miyagishima SY. Mechanism of plastid division: from a bacterium to an organelle. Plant Physiol. 2011; 155(4):1533–1544. [PubMed: 21311032]

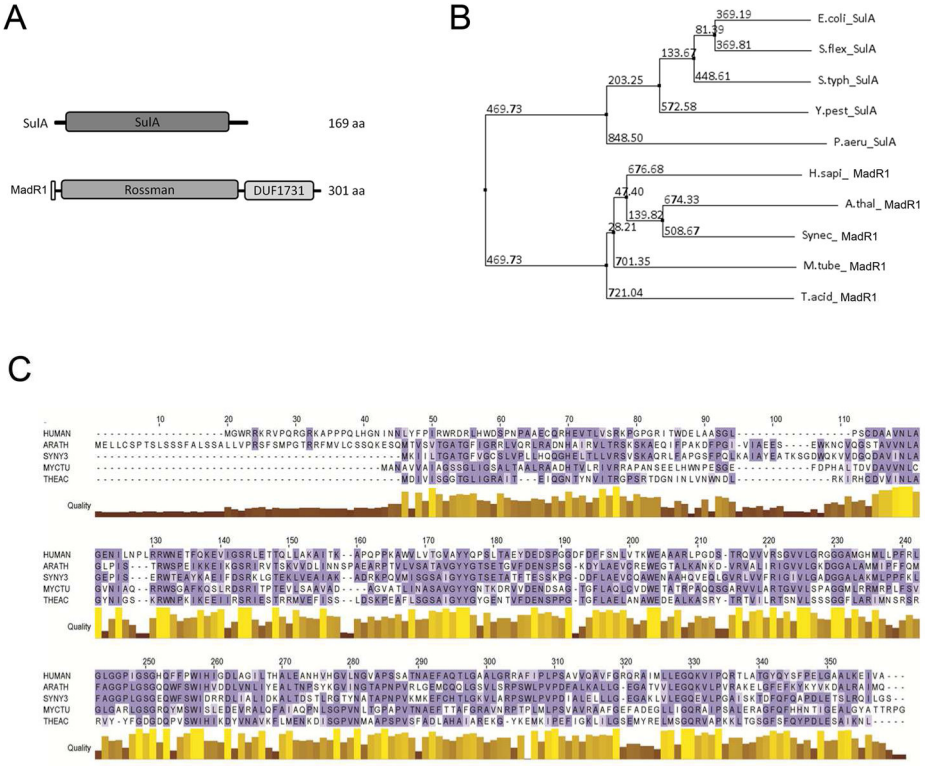

Figure 1. Defining the MadR1 protein family

(A) Select MadR1 proteins were chosen from among the predicted 561 orthologs to visualize sequence conservation in species from different kingdoms. Shared amino acids are indicated by dark blue shading, non-identical residues sharing similar biochemical properties are indicated by light blue shading. Quality scores on the alignment indicate the probability that the observed amino acids in a given aligned column are the result of conserved or favorable features, with a lower score indicating good potential for mutation or unfavorable mutation, and higher scores posing less cost. MadR1 proteins derived from: HUMAN - *Homo sapien* [UniProt accession no. **Q9NRG7**]; ARATH - *Arabidopsis thaliana* [UniProt accession no. **Q9SJU9**]; SYNCY - *Synechocystis* sp. PCC6803 [UniProt accession no. **P73467**]; MYCTU - *Mycobacterium tuberculosis* [UniProt accession no. **P67232**]; and THEAC - *Thermoplasma acidophilum* [UniProt accession no. **Q9HIQ8**].. Quality scores on the alignment indicate the probability that the observed amino acids in a given aligned column are the result of conserved or favorable features, with a lower score indicating good potential for mutation or unfavorable mutation, and higher scores posing less cost. (B) Neighbor-joining tree showing the predicted phylogenetic relationship between diverse MadR1 and SulA proteins. Tree branch lengths correspond to distance values based upon the original multialignment and are minimized during tree construction. Phylogenetic annotations of MadR1 proteins described above for 1-A. SulA proteins from bacteria: E.coli – *Escherichia coli* [UniProt accession no. **P0AFZ5**]; S.flex – *Shigella flexneri* [UniProt accession no. **Q0T677**]; S.typh – *Salmonella typhi* [UniProt accession no. **P0A241**]; Y.pest – *Yersinia pestis* [UniProt accession no. **Q7CHL5**]; and P.aeru – *Pseudomonas aeruginosa*

[UniProt accession no. **Q9HZJ8**]. (C) Protein functional domains maps of MadR1 and SulA family proteins.

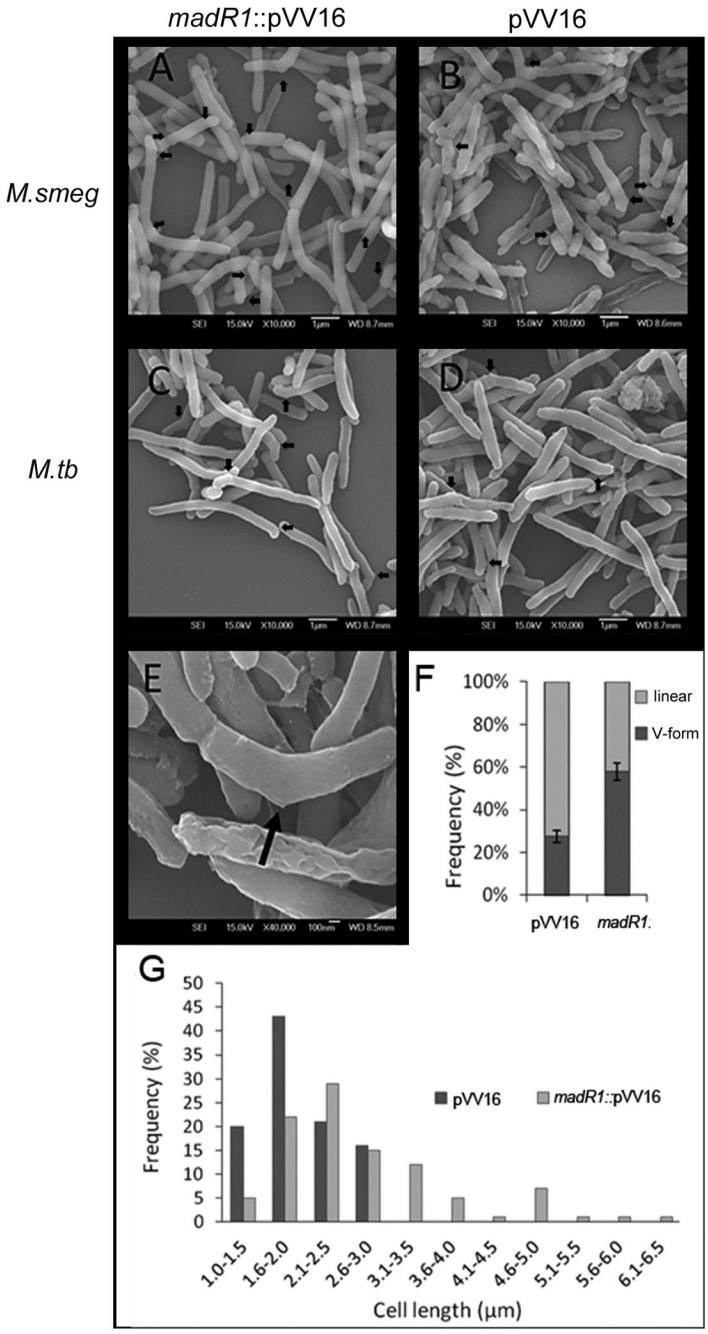

Figure 2. SEM morphological analysis for induced expression of *madR1*

Scanning electron microscopy of (A) *M. smegmatis madR1*:pVV16, (B) *M. smegmatis* pVV16 vector control, (C) *Mtb madR1*:pVV16 and (D) *Mtb* pVV16 vector control strains. Example of V-form type of bent cell morphology (E and black arrows). (F) Relative frequency of V-form and linear morphologies per 100 cells at mid log growth. Brackets indicate standard error among counts from 5 replicate fields of view; asterisks indicate a statistically significant difference between the relative proportions of morphologies for the

two strains by Pearson's chi-squared test with a p-value of 1.56e-5. (G) Frequency of cell lengths in *madR1* merodiploids compared to vector control cells.

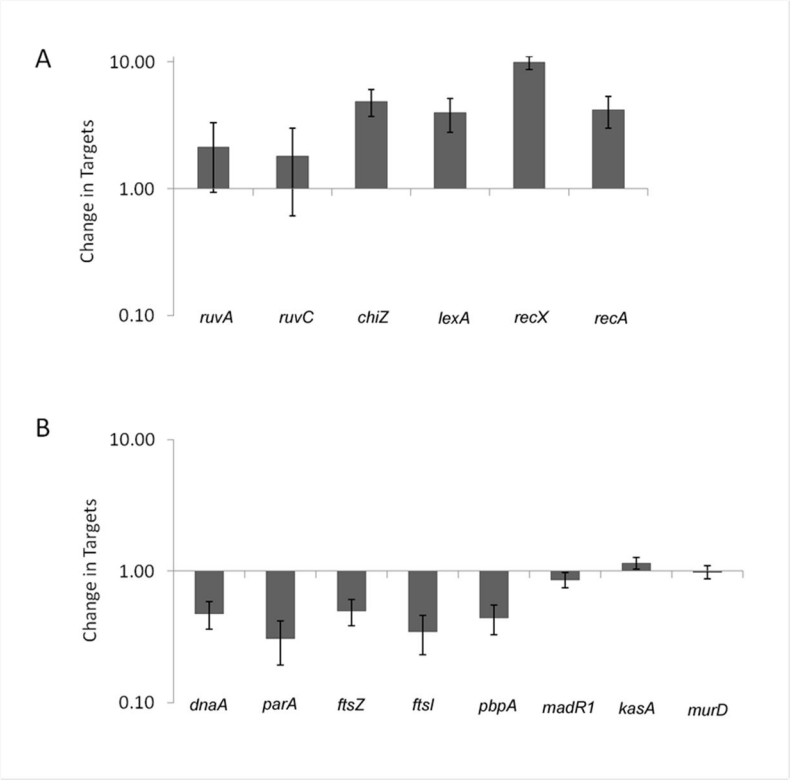

Figure 3. Effects of DNA damage on *Mtb* transcription

qRT-PCR expression profiles obtained for select (A) SOS response genes and (B) cell division genes in *Mtb* following Mitomycin C-mediated DNA damage. Values are displayed as an average log2-transformed change in expression after 24 hour Mitomycin C treatment, relative to un-treated controls. Brackets indicate standard error calculated from 3 replicates.

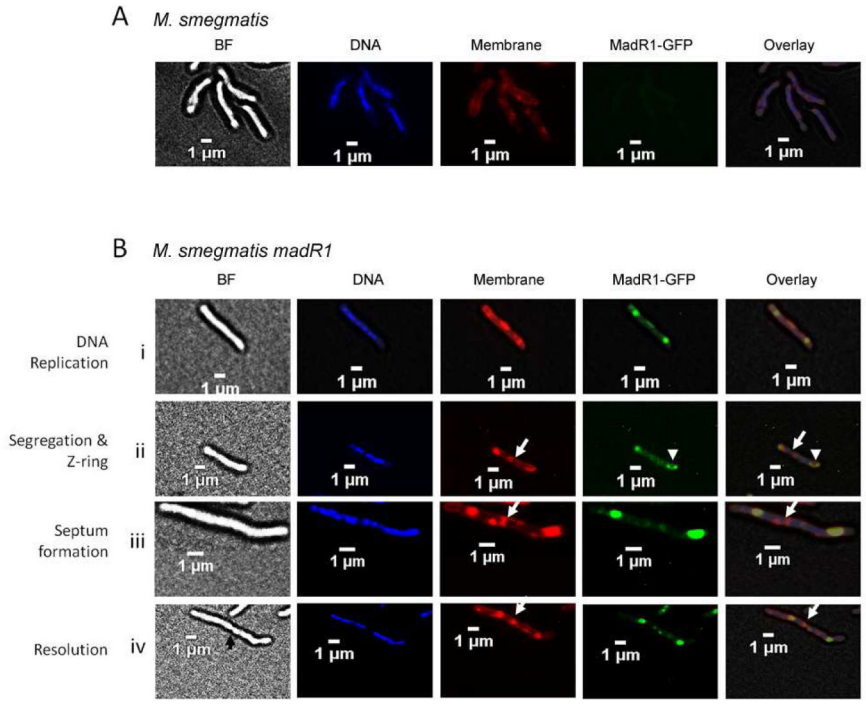

Figure 4. Localization of MadR1-GFP in *M. smegmatis*

Fixed cell microscopy of (A) wild type *M. smegmatis* and (B) *madR1*::pMCSU7 strain expressing MadR1-GFP sorted by progression through the division cycle: (i) early division, (ii) segregation & Z-ring formation, (iii) septum formation and (iv) resolution. Membranes stained with FM 4–64 Fx appear red, DNA stained with DAPI is blue and MadR1- GFP is green. Bright field microscopy (BF). All images taken at 1000x magnification White full arrow indicates the division site, white arrowhead highlights the peculiar activity of MadR1-GFP at the developing vertex of future V-form cell, black full arrow showing the early division furrow.

Table 1

Functional enrichment of the 277 ORFs displaying a ≥ 2-fold change in expression, using three different gene ontology algorithms.

Ontology Groups UP	# ORFs in Profile (%)	# ORFs in Genome (%)	Corrected p-value
Gene Ontology (GO)			
Growth	14 (6.1)	621 (15.5)	0
Plasma membrane	47 (20.4)	1284 (32.1)	0.002
Categories of Orthologous Groups (COG)			
Lipid transport and metabolism	18 (13.1)	263 (6.5)	0.04
Secondary metabolite biosynthesis, transport & catabolism	17 (12.4)	240 (6)	0.04
Pathway Ontology			
Fatty acid and beta oxidation I	4 (20)	39 (1)	0
Lactate oxidation	2 (10)	7 (0.2)	0.007
Histidine biosynthesis I	2 (10) 8 (0.2)		0.009
Pyruvate dehydrogenase complex I	2 (10)	8 (0.2)	0.009

Ontology Groups DOWN	# ORFs in Profile (%)	# ORFs in Genome (%)	Corrected p-value
Gene Ontology			
NADH dehydrogenase (ubiquinone)	5 (3.2)	14 (0.4)	0.009
Plasma membrane	26 (15.6)	1284 (32.1)	0
COG Categories			
Energy production and conservation	12 (20)	218 (5.5)	0.001
Pathway Ontology			
Resp. (anaerobic) - electron donors	5 (20)	18 (0.5)	0
Fatty acid biosynthesis - initial steps	2 (8)	9 (0.2)	0.02
Fatty acid elongation - unsaturated I	2 (8)	6 (0.2)	0.009
Tryptophan biosynthesis	2 (8)	6 (0.2)	0.009